



HHS Public Access

Author manuscript

Small. 2011 March 21; 7(6): 727–731. doi:10.1002/sml.201002186.

Published in final edited form as:

Small. 2011 March 21; 7(6): 727–731. doi:10.1002/sml.201002186.

Hybrid Top-Down and Bottom-Up Fabrication Approach for Wafer-Scale Plasmonic Nanoplatfoms

Dr. Anuj Dhawan,

Fitzpatrick Institute for Photonics, Departments of Biomedical Engineering and Chemistry, Duke University, Durham, NC, USA. Electronics Division, US Army Research Office, Research Triangle Park, Durham, NC, USA

Dr. Yan Du,

Department of Electrical & Computer Engineering, NC State University, Raleigh, NC, USA

Dr. Dale Batchelor,

Department of Materials Science and Engineering, NC State University, Raleigh, NC, USA

Hsin-Neng Wang,

Fitzpatrick Institute for Photonics, Departments of Biomedical Engineering and Chemistry, Duke University, Durham, NC, USA

Dr. Donovan Leonard,

Department of Physics and Astronomy, Appalachian State University, Boone, NC, USA

Prof. Veena Misra,

Department of Electrical & Computer Engineering, NC State University, Raleigh, NC, USA

Prof. Mehmet Ozturk,

Department of Electrical & Computer Engineering, NC State University, Raleigh, NC, USA

Dr. Michael D. Gerhold, and

Electronics Division, US Army Research Office, Research Triangle Park, Durham, NC, USA

Prof. Tuan Vo-Dinh

Fitzpatrick Institute for Photonics, Departments of Biomedical Engineering and Chemistry, Duke University, Durham, NC, USA

Bridging the nanoscale level of probe fabrication and the megascale dimensions of sensor systems is one of the greatest challenges in the development of large-area plasmonic sensing platforms. We report a generalized hybrid nanofabrication approach combining top-down (deep-UV lithography) and bottom-up (controlled lateral epitaxial growth and atomic layer deposition) fabrication techniques for the development of nanostructured platforms. This technology allows the development of reproducible substrates with controlled sub-10 nm gaps between plasmonic nanostructures over an entire 6 inch wafer (1 inch \approx 2.54 cm). By integrating soft matter (DNA probes) and hard matter (silicon nanochips), these

Correspondence to: Tuan Vo-Dinh.

Supporting Information

Supporting Information is available from the Wiley Online Library or from the author.

nanoplatfoms can be employed in a wide variety of applications ranging from chemical detection to biosensing. To illustrate their usefulness in biosensing, the nanoplatfoms are used for detecting biochemical species and labeled breast cancer DNA molecules using surface-enhanced Raman scattering.

Plasmonics, which refers to the research area of enhanced electromagnetic fields in the vicinity of metallic thin films and nanostructures, has led to the development of extremely sensitive optical detection techniques, such as surface plasmon resonance (SPR) and surface-enhanced Raman scattering (SERS). In recent years, the SERS technique has become a powerful spectroscopic tool for the nondestructive detection of a wide variety of compounds of chemical, biological, and medical interest.^[1–11] Raman spectra exhibit narrow spectral features characteristic of the detected analyte species, allowing the specific detection of these species. Research efforts have been devoted to maximizing SERS signals from molecules located inside or near nanoscale gaps between plasmonically active metallic nanostructures on the SERS substrates.^[12–15] In spite of these advances, the scaling process that bridges the gap from the nanoscale requirements of SERS-active structures to the macroscale dimensions (e.g., wafer size) of practical sensors is a great challenge. In this paper, we describe a novel hybrid approach—employing both bottom-up and top-down fabrication methodologies (see Figure 1)—for developing well-controlled 1D and 2D periodic, plasmonically active, diamond-shaped, nanowire structures with sub-10 nm gaps. We apply these novel plasmonic substrates for SERS detection of biochemical species and labeled breast cancer DNA molecules, thereby demonstrating a class of plasmonic biosensors that could be developed on a wafer scale.

A unique plasmonic nanostructure based on diamond-shaped nanowires (DNWs) containing sub-10 nm gaps is described in this work. The nanoscale gaps developed between the diamond-shaped nanowires can produce high electromagnetic (EM) field enhancement, and therefore high SERS EM enhancement,^[1,16,17] if the nanowire structures are tuned to plasmon resonance wavelengths associated with the nanostructures. Plasmonically active SERS substrates based on metallic nanogratings allow the direct coupling of normally incident radiation (transverse magnetic polarization) to surface plasmons without the need of any coupling mechanism (e.g., prism coupling). A theoretical description of plasmonic enhancement of EM fields in metallic nanogratings (i.e., between nanolines in gratings), and correlation of the EM fields to SERS enhancement factors, is provided in the Supporting Information (SI), sections S1 and S2. DNWs (cross-sectional schematic shown in Figure 2A) can be continuous 1D lines (see SI, section S3) or have a 2D structure with individual nanowires of a subwavelength dimension (see Figure 2B and SI, section S4). The development of 2D metal-coated nanowires could lead to the enhancement of EM fields in two directions—in the gaps between the nanowires and in the gaps along the nanowire length—when unpolarized light is employed, thereby leading to a higher density of SERS hotspots (see SI, section S4). In our work a hybrid fabrication approach is followed that combines 1) deep-UV lithography (which traditionally cannot be employed for developing silicon nanostructures and nanoscale gaps smaller than ≈ 60 nm) for developing silicon nanostructures with 2) controlled epitaxial growth of silicon–germanium on certain facets of silicon nanostructures to controllably reduce gap between nanostructures, as well as 3) atomic layer deposition and metal evaporation. This unique fabrication procedure involving

lateral epitaxial silicon–germanium growth allows us to controllably reduce gaps between adjacent nanowires, which are then coated with plasmonically active metals to obtain metal-coated nanowires with sub-10 nm gaps. To our knowledge, sub-10 nm gaps between plasmonically active nanostructures have not been achieved controllably on a wafer scale by other nanofabrication processes.

In our work, the first fabrication step involved the development of silicon nanowires on a 6 inch wafer (See SI, section S3). Silicon and silicon-on-insulator (SOI) wafers were patterned using a combination of deep-UV lithography (193 nm UV lithography using ASML 5500/950B Scanner) and dry etching (reactive ion etching). This enabled the development of silicon nanowires of varying sizes and spacings (100 nanometers to 10 micrometers) between the wires over the entire 6 inch wafer. We also employed 20–40 nm wide silicon nanowires patterned by SEMATECH consortia (using deep-UV lithography) on commercial SOITECH silicon on insulator (SOI) wafers, with a 150 nm buried oxide layer.

To develop DNW structures, silicon–germanium ($\text{Si}_{1-x}\text{Ge}_x$) epitaxial films were grown on the silicon nanowires using the ultra-high vacuum rapid thermal chemical vapor deposition process and then over-coated with a layer of a plasmonically active metal such as silver or gold. This bottom-up approach, based on controlled directional epitaxial growth, led to the unique diamond-shaped structures of the $\text{Si}_{1-x}\text{Ge}_x$ nanowires and enabled the size of the gap between the nanowire structures to be precisely controlled. In the epitaxial growth of $\text{Si}_{1-x}\text{Ge}_x$ on silicon nanowires patterned on (100) silicon wafers, at 550 °C growth temperature, (111) facet formation was dominant (details in SI, section S3). Between two parallel $\text{Si}_{1-x}\text{Ge}_x$ DNWs, one can observe small triangular sections (see transmission electron microscopy (TEM) cross-sections of $\text{Si}_{1-x}\text{Ge}_x$ DNWs in Figure 2C, D, x being 0.28) that are formed due to $\text{Si}_{1-x}\text{Ge}_x$ growth on the bottom silicon region between the lithographically formed silicon nanowires. One can observe sub-10 nm gaps between the gold-coated nanostructures present in the DNW substrates (see Figure 2C, D), which can lead to a large enhancement of EM fields in these regions. Figure 2E, F show TEM cross-sections of silicon–germanium nanowires grown on an SOI substrate. In Figure 2E, one does not observe the triangular sections between the diamond-shaped nanowires as there is no silicon layer present at the bottom of the silicon nanowires developed on top of the buried oxide layer of the SOI wafers. The high-resolution TEM image shown in Figure 2F shows the crystal planes of the epitaxially grown $\text{Si}_{1-x}\text{Ge}_x$ nanowires. Although the diamond-shaped cross-sectional geometry shown in Figure 2D does not have pointed diamonds, the $\text{Si}_{1-x}\text{Ge}_x$ nanowires shown in Figure 2E (developed on SOI wafers) had a sharp, diamond-shaped geometry. This illustrates our capability of developing pointed geometries of diamond-shaped nanowires that could be applied for further concentration and enhancement of EM fields between the tips of the metal-coated diamond nanostructures (or between diamond and triangular nanostructures), potentially leading to further enhancement of SERS signals from molecules lying in this region. The lateral growth of the diamond-shaped nanostructures, for both kinds of DNWs shown in Figure 2D, E, can be carried out until the desired gap is achieved such that the final gap after plasmonic metal deposition is sub-10 nm. Potentially, even sub-5 nm gaps can be achieved. In the final fabrication process, the plasmonically active substrates were developed by over-coating the DNW structures with a

20–100 nm thick film (see Figure 2A–D) of plasmonically active metals (such as gold or silver) using sputtering or electron beam evaporation (details in SI, section S3).

Another bottom-up fabrication methodology, atomic layer deposition (ALD), can be employed in conjunction with the epitaxial silicon–germanium growth to reduce the gaps between neighboring silicon–germanium nanowires before the final over-coating with the plasmonically active metals is carried out. ALD can be employed to develop a conformal spacer layer of a dielectric material or platinum (cross-section TEM image shown in Figure 2E), such that the narrow gaps between the diamond-shaped nanowires could be further reduced in a controllable manner. The current ALD technology allows deposition of conformal platinum thin films, but not of plasmonically active metals such as gold, silver, or copper. Since transition metals such as platinum exhibit weaker plasmonic properties in the visible spectral region than coinage noble metals—due to the large imaginary part of their dielectric constant—they (e.g., ALD deposited platinum) can't be employed for developing the plasmonically active metal layer on the nanowires. Future improvements in ALD technology could enable ALD to be employed not only for developing the spacer layer for reducing the gaps between the nanostructures but also for the conformal deposition of plasmonically active metals such as copper^[18] and possibly also gold and silver.

We performed numerical calculations using the finite difference time domain (FDTD) method (calculation details in the SI, section S2) to determine the electric field enhancement in the nanoscale gaps in the DNW substrates. In our calculations, gold-coated diamond-shaped silicon nanowires were simulated as shown in Figure 3A. Figure 3B–E indicate that the E-field enhancement (enhancement of the electric field as a function of the incident field) increases from ≈ 7.6 to 18.5 (for 633 nm wavelength incident radiation) and from ≈ 9.5 to 25.6 (for 785 nm wavelength incident radiation) when the minimum spacing between the gold-coated diamond-shaped silicon nanowires and the triangular nanowire structures between them is reduced from 20 to 4 nm. One can also observe enhancement of EM fields in the gap regions between the diamond-shaped nanowires and the triangular nanowires that are present towards the bottom of the nanowires, i.e., towards the silicon substrate (see Figure 3B–E and Figure 2A). As the SERS EM enhancement is approximately equal to the fourth power of the electric field enhancement, the results shown in Figure 3B–E indicate that decreasing the space between the diamond-shaped nanowires and the triangular nanowires can lead to an increase in the SERS EM enhancement of molecules in the region between the nanowires.

To illustrate the usefulness of the DNW plasmonic platforms, we performed SERS measurements using nanowire substrates—SERS-active DNW substrates (Figure 3F) developed on a wafer scale (Figure 3G)—coated with chemical dyes such as p-mercaptobenzoic acid (pMBA), and compounds of chemical or biomedical interest. The presence of chemical and biological molecules in the SERS hotspots *H* shown in Figure 2A can lead to significant enhancement of SERS signals from these regions, thereby enabling the detection of very low concentrations of these molecules.

Figure 3H shows SERS spectra, obtained from 1 mM of pMBA molecules adsorbed onto the DNW substrates, that exhibit strong Raman bands at 1590 and 1080 cm^{-1} , corresponding to

ν_{8a} and ν_{12} aromatic ring vibrations, respectively. Figure 3H shows that the intensity of the 1590 cm^{-1} SERS peak is $\approx 63\,000$ counts for the DNWs having $\approx 80\text{ nm}$ spacing between the nearest ends of diamond-shaped nanowires, with small triangular structures lying in between the nanowires. The high SERS signals obtained from these DNWs can be explained by the presence of very small nanoscale gaps (slightly less than 10 nm) between the metallic nanostructures in the DNW substrates (see Figure 2C, D). This is in accordance with the FDTD calculations that describe EM field enhancement in the nanoscale gaps in the DNWs (see Figure 3B–E). The calculations show an increase in the field enhancement as the smallest gap between the nanowires is reduced. Moreover, there was $\approx 10^7$ times enhancement of SERS signals for the DNW regions as compared with continuous gold film regions. Figure 3I shows the application of DNW SERS substrates for SERS detection of dipicolinic acid, a biomarker for spores of bacteria such as Anthrax (*Bacillus anthracis*) (see SI, section S5, for details). Figure 3J shows SERS signals obtained from a dye-labeled breast cancer DNA sequence (ERBB2 or v-erb-b2 erythroblastic leukemia viral oncogene homolog 2, a neuro/glioblastoma-derived oncogene homolog (avian)) having the SERS-active dye Cy3 covalently bound at the end of the DNA molecules. When Cy3 dye-labeled gene segments were delivered to the gold-coated nanowire substrate in a buffer solution (shown in Figure 3B), one could observe intense SERS signal exhibiting Raman peaks at 1588 , 1469 , 1406 , 1393 , and 1270 cm^{-1} (see Figure 3J).

This study demonstrates the possibility of using a hybrid approach (top-down and bottom-up) for the large-scale fabrication of controlled and reproducible plasmonically active substrates with sub- 10 nm gaps between metallic nanowire structures on entire silicon wafers; an achievement which has not been accomplished controllably on a wafer scale by other nanofabrication processes. These gap regions between plasmonic nanostructures act as SERS hotspots for molecules lying there, thereby enabling the SERS-based detection of low concentrations of these molecules. The results of this study lay the foundation for development of nanochip-based chemical and biological sensors on a wafer scale, such that biochemical species (e.g., DNA molecules associated with various diseases) could be detected with high levels of sensitivity and specificity. By bridging the nanoscale level of probe structures with the micromillimeter-scale dimension of sensor systems, this approach opens new horizons to more widespread applications in chemical sensing and biomedical diagnostics.

Experimental Section

SERS Measurements

SERS measurements were performed using a Renishaw InVia Raman system that consists of a 50 mW , HeNe laser (632.8 nm laser line, Coherent, Model 106–1) as the excitation source. A 1800 groove-per-mm grating was employed to obtain a spectral resolution of 1 cm^{-1} . Raman scattering was detected by a $1024\text{ pixel} \times 256\text{ pixel}$ RenCam charge-coupled device detector. The SERS spectra were acquired with a 10 s integration time and processed with software from Renishaw (WiRE 2.0).

Microliter samples of analyte solutions—Raman-active dyes such as p-mercaptobenzoic acid (pMBA), dye mixtures, and compounds of chemical or biological interest—were

delivered to the substrates and either the solvent was allowed to dry for SERS measurements or a washing step was employed to remove the molecules that were not attached to the substrate. In the case of pMBA, the substrates were dipped in an ethanol solution of pMBA (1 μ M to 1 mM), followed by a rinse in pure ethanol for washing of pMBA molecules that have not bonded to the DNWs, and finally drying ethanol by flowing nitrogen.

Labeled DNA Detection

In order to demonstrate the applicability of the DNW substrates to biomedical sensing, these substrates were employed for SERS detection of Raman-labeled ERBB2 gene, which is known as a key biomarker for breast cancer. The DNA sequences were synthesized by IDT (Integrated DNA technologies, Coralville, IA). To carry out the labelled DNA detection, two microliters of a Cy3 dye-labeled gene (ERBB2 DNA) segment (1 μ M solution) in a buffer (0.5 M NaCl, 10 mM sodium phosphate buffer) was delivered to the gold-coated nanowire substrates and the SERS spectra obtained on the dried samples. We also employed a molecular printer called Nano eNabler to pattern chemical and biological analyte molecules on the DNW chips (details are in the SI, section S6).

TEM and SEM Imaging

TEM images were taken in a Hitachi HF2000 Transmission Electron Microscope. Sample preparation for obtaining the TEM cross-section of the DNWs was carried out using a focused ion beam machine (FEI, Inc. Quanta 200 3D Dual Beam FIB). SEM images were taken on a JEOL 6400F Field Emission SEM.

Supplementary Material

Refer to Web version on PubMed Central for supplementary material.

Acknowledgments

The authors would like to thank the sponsors of this work – US Army Research Office, National Research Council, and the National Institutes of Health (Grants R01 EB006201 and R01 ES014774). We would also like to thank Dr. Harris at SEMATECH consortia for providing support for this work.

References

1. Otto A, Mrozek I, Grabhorn H, Akemann W. *J Phys: Condens Mat.* 1992; 4:1143.
2. Moskovits M. *Rev Mod Phys.* 1985; 57:783.
3. Chang, RK., Furtak, TE., editors. *Surface-Enhanced Raman Scattering.* Plenum; New York: 1982.
4. Fleischmann M, Hendra PJ, McQuillan AJ. *Chem Phys Lett.* 1974; 26:163.
5. Jeanmaire DL, Van Duyne RP. *J Electroanal Chem.* 1977; 84:1–20.
6. Albrecht MG, Creighton JA. *J Am Chem Soc.* 1977; 99:5215.
7. Vo-Dinh T, Hiromoto MYK, Begun GM, Moody RL. *Anal Chem.* 1984; 56:1667.
8. Cao YC, Rongchao J, Mirkin CA. *Science.* 2002; 297:1536. [PubMed: 12202825]
9. Vo-Dinh T. *Trends Anal Chem.* 1998; 17:557.
10. Nie S, Emory SR. *Science.* 1997; 275:1102. [PubMed: 9027306]
11. Xu H, Bjerneld EJ, Kall M, Borjesson L. *Phys Rev Lett.* 1999; 83:4357.
12. Qin L, Zou S, Xue C, Atkinson A, Schatz GC, Mirkin CA. *Proc Natl Acad Sci USA.* 2006; 104:13300.

13. Cui B, Clime L, Li K, Veres T. *Nanotechnology*. 2008; 19:145302. [PubMed: 21817756]
14. Liu GL, Lee LP. *Appl Phys Lett*. 2005; 87:074101.
15. Wang HH, Liu CY, Wu SB, Liu NW, Peng CY, Chan TH, Hsu CF, Wang JK. *Adv Mater*. 2006; 18:491.
16. Kerker M. *Acc Chem Res*. 1984; 17:271.
17. Aravind PK, Metiu H. *Chem Phys Lett*. 1980; 74:301.
18. Lim BS, Rahtu A, Gordon RG. *Nature Mat*. 2006; 2:749.

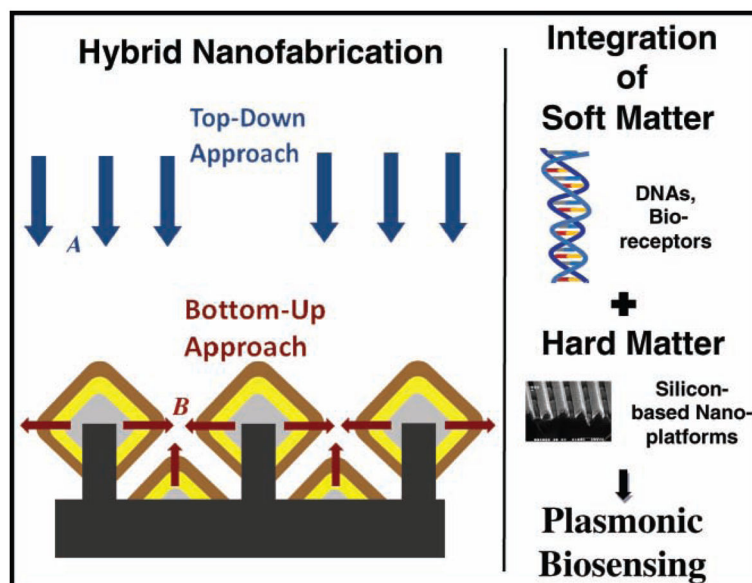


Figure 1. Schematic illustrating the development of novel, plasmonically active, diamond-shaped nanowire structures employing a hybrid approach combining the top-down methodologies *A* (deep-UV lithography, dry etching, and metal evaporation) with bottom-up methodologies (epitaxial silicon–germanium growth, including lateral diamond-shaped silicon–germanium nanowire growth *B* that bridges the gaps between the nanowires and the development of triangular nanostructures between the diamond-shaped nanostructures, as well as atomic layer deposition), such that chips containing these nanowire structures could be employed for plasmonics-based sensing of chemical and biological molecules.

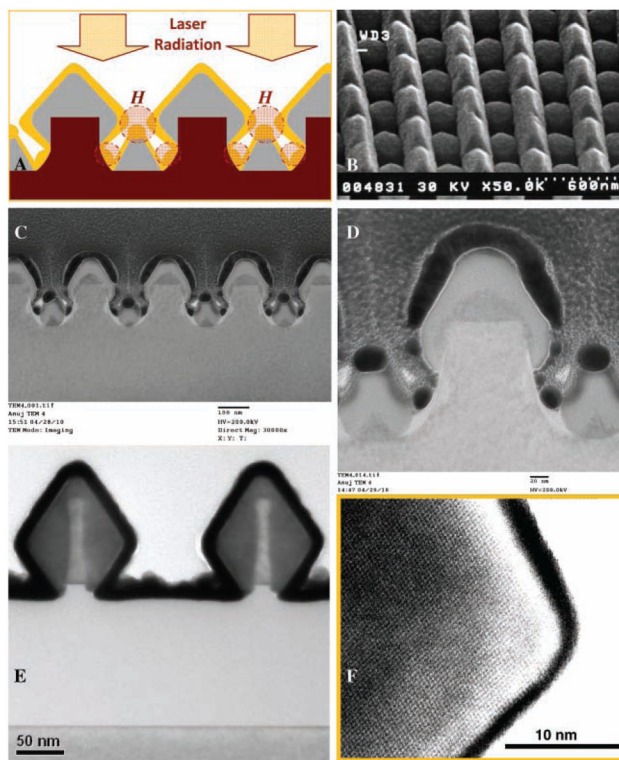


Figure 2.

A) Schematic of $\text{Si}_{1-x}\text{Ge}_x$ nanowires (light grey color) with a diamond-shaped structure, epitaxially grown from silicon nanowires (magenta color). The $\text{Si}_{1-x}\text{Ge}_x$ nanowires were coated with gold film (yellow color). When laser radiation is incident on the gold-coated DNWs, SERS hotspots H are produced between the diamond-shaped and the triangular nanowire structures. B) Scanning electron microscopy (SEM) image of 2D gold-coated $\text{Si}_{1-x}\text{Ge}_x$ nanowires. C, D) TEM cross-section image showing small triangular sections formed in between the diamond NWs. E) TEM cross-section image showing ALD of platinum (black color) on the diamond-shaped $\text{Si}_{1-x}\text{Ge}_x$ nanowires (dark grey color) formed on SOI wafers. F) High-resolution TEM image of the $\text{Si}_{1-x}\text{Ge}_x$ nanowires.

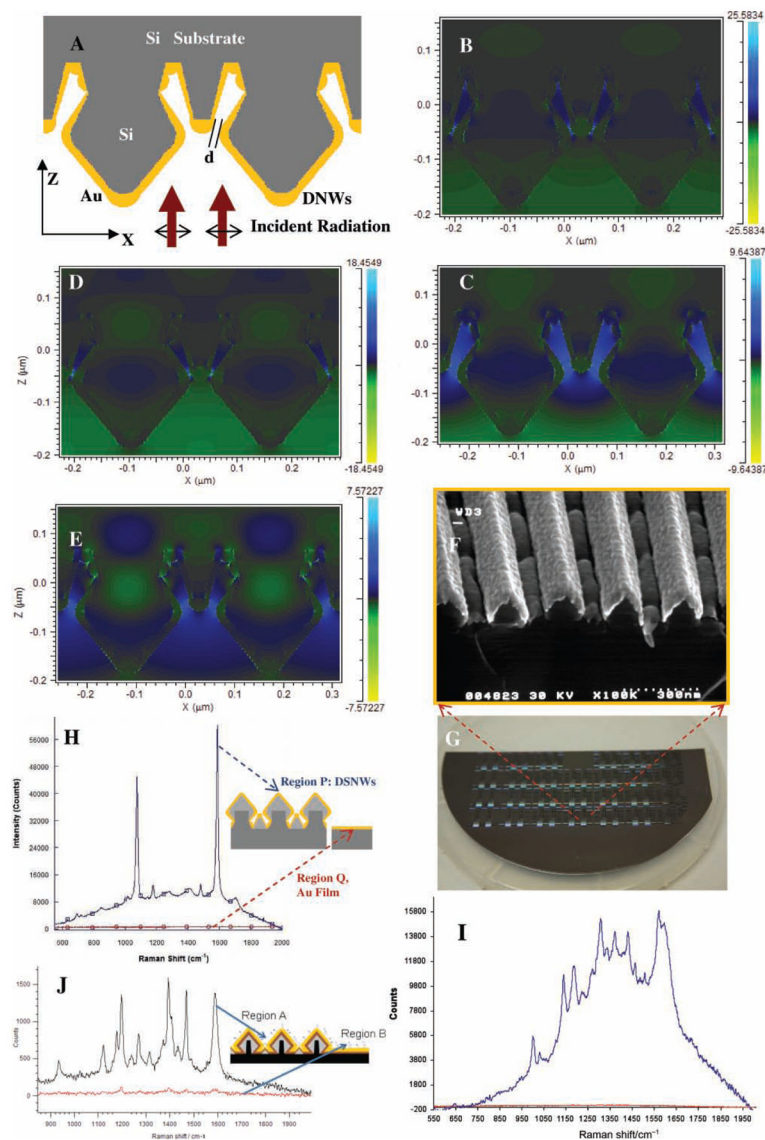


Figure 3.

A) Schematic of the gold-coated silicon nanowire structures simulated using 2D FDTD calculations. Simulations show enhancement of the electric field in the spaces between the diamond-shaped nanowires and the triangular nanowires. B–E) Enhancement of electric field when the nearest spacing ‘d’ between adjacent tips of diamond-shaped and triangular nanowires is B) 4 nm and C) 20 nm, with 785 nm radiation normally incident on the nanowires, and D) 4 nm and E) 20 nm with 633 nm radiation incident on the DNW structures. F) SEM micrograph of 1D gold-coated $\text{Si}_{1-x}\text{Ge}_x$ nanowires. G) Part of a 6 inch SERS substrate wafer with nanowire structures. H) SERS signals from 1 mM pMBA (in blue) on gold-coated DNW substrates as compared to that from a gold film (red). I, J) SERS signals from gold-coated DNW substrates showing detection of I) 80 ppm DPA (signal from DNW region P in blue, and from planar gold film region Q in red), J) 1 μM Cy3 dye-labeled

ERBB2 DNA segment solution (region A, in black), as compared with SERS signal from gold region with no nanowires (region B, in red).

Author Manuscript

Author Manuscript

Author Manuscript

Author Manuscript